

## Synthesis, Vibrational Spectroscopic and Thermal Properties of Oxocarbon Cross-Linked Chitosan

Nelson L. G. D. Souza,<sup>a</sup> Tamyres F. Salles,<sup>a</sup> Humberto M. Brandão,<sup>b</sup>  
Howell G. M. Edwards<sup>c</sup> and Luiz F. C. de Oliveira<sup>\*a</sup>

<sup>a</sup>Núcleo de Espectroscopia e Estrutura Molecular (NEEM), Departamento de Química,  
Universidade Federal de Juiz de Fora, 36036-900 Juiz de Fora-MG, Brazil

<sup>b</sup>Empresa Brasileira de Pesquisa Agropecuária, Centro Nacional de Pesquisa de Gado de Leite,  
36038-330 Juiz de Fora-MG, Brazil

<sup>c</sup>Centre for Astrobiology and Extremophile Research, School of Life Sciences,  
University of Bradford, BD7 1DP Bradford, United Kingdom

In this work specimens of chitosan which have been cross-linked covalently and ionically with different oxocarbon and pseudo-oxocarbon anions have been synthesised and characterized using infrared and Raman spectroscopic techniques, solid state <sup>13</sup>C nuclear magnetic resonance (NMR) and by thermogravimetry. According to the spectroscopic and thermal results, ionically crosslinked chitosans are obtained with squarate, croconate and rhodizonate ions as crosslinking agents, whereas covalently crosslinked chitosan can be obtained when squaric acid is used as the crosslinking agent; the same products are not observed when the pseudo-oxocarbon anion croconate violet is used, which can be attributed to the low basic strength of the crosslinking species.

**Keywords:** chitosan, crosslinking, oxocarbon, infrared and Raman, solid state <sup>13</sup>C NMR

### Introduction

Chitosan is a copolymer of β-(1→4)-linked 2-acetamido-2-deoxy-D-glucopyranose and 2-amino-2-deoxy-D-glucopyranose.<sup>1</sup> This polycationic biopolymer can be obtained by partial deacetylation of chitin extracted from crustaceans.<sup>2</sup> The main parameters influencing the characteristics of chitosan are its molecular weight (MW) and degree of deacetylation (DD), representing the proportion of deacetylated units. These properties can be modified<sup>3</sup> as follows: the DD can be lowered by reacylation<sup>4</sup> and the MW can be lowered by acidic depolymerisation.<sup>5</sup>

Chitosan has attracted much attention mainly due to its potential biological applications, which include a unique antichloristic effect, bio-compatibility, absorptivity, non-hypersensitivity, biodegradability and a significant wound healing ability.<sup>6-9</sup> Due to these properties this polymer has been used in several different applications, such as drug and gene delivery vehicles,<sup>10</sup> tissue engineering scaffolds<sup>11</sup> and in wound dressings.<sup>12</sup> In the medical sciences area, chitosan has been used in optical ocular applications,<sup>13</sup> tissue

implantations<sup>14</sup> and injections,<sup>15</sup> as well as its properties of wound-healing<sup>16</sup> and bacteriostasis mentioned earlier.<sup>17,18</sup> The ready availability of chitosan coupled with its low cost production is of interest ecologically, which further enhances its potential applications in materials science. In the search for novel applications for this versatile natural polymer, its chemical modification is desirable to enhance its stability in acidic media, to decrease its solubility in mineral and organic acids and to increase its resistance to biochemical and biological degradation. However, these chemical modifications can sometimes only be achieved at the expense of a decreased thermal stability and the purpose of this study is to evaluate the potential improvements in the chemical behavior against any observed detrimental factors in the thermal properties of a range of crosslinked chitosan polymers.

Cross-linking is a procedure used to carry out synthetic modifications to polymer chains to provide designed properties such as those described above by which the molecular weight can be increased and novel functionalities introduced into the hybrid networks to facilitate desired solubilities.<sup>3</sup> The crosslinking procedure involves the chemical reaction between specific sites present in the

\*e-mail: luiz.oliveira@ufjf.edu.br

structural units of chitosan and the selected cross-linking reagents. In the case of chitosan, the hydroxyl and amino groups are the most reactive sites for cross linking reactions to be undertaken on the parent natural polymer in order to modify its chemical and thermal stability, structural rigidity, permeability, color, chelation capacity and efficiency in immobilization of cellular proteins,<sup>19</sup> all of which are desirable adaptations for future biomedical applications.

Several covalent cross-linking agents such as glyoxal,<sup>20</sup> formaldehyde,<sup>21</sup> benzoquinone,<sup>10</sup> nitrilotriacetic acid<sup>22</sup> and epichlorohydrin<sup>23</sup> have already been proposed for chitosan modification, but glutaraldehyde is the most widely used because it does not present a decrease in adsorption capacity which is a result of crosslinking experiments with the other reagents.<sup>24</sup> In addition to covalent cross-linked chitosan polymers there is also the possibility of making ionic crosslinked chitosan in the presence of agents such as phosphates, citrates and sulfates.<sup>25-27</sup>

In this respect, a class of compounds which can be used as novel cross-linking agents for chitosan are the oxocarbons which have the versatility of being able to produce both covalent and ionic crosslinked chitosan polymer products from which the influence of the ionic and covalent crosslinking synthetic procedures involving the same family of reactants on the polymer products can be evaluated for the first time. The parent oxocarbon of the family being discussed here is represented by the general formula,  $H_2C_nO_n$ , and the anions are cyclic compounds,  $(C_nO_n)^{-2}$ , where n varies from 3 (deltate), 4 (squarate), 5 (croconate) to 6 (rhodizionate), each molecule and molecular ion of which has some unusual electronic and vibrational properties (Figure 1)<sup>28</sup> which could be imparted to novel polymers through their participation in crosslinked chitosan. Partial or complete replacement of the carbonyl oxygen atoms by sulfur, selenium or dicyanomethylene

groups leads to the formation of derivatives, the so-called pseudo-oxocarbons.<sup>29</sup>

Oxocarbon ions are employed as photoreceptors and semiconductor materials having non-linear optical properties;<sup>30</sup> rhodizonate salts are widely used as analytical reagents, for example, in the identification of traces of lead in the criminal forensics area, as well as providing evidence for the identification of iron(II) and barium ions.<sup>31</sup> Rhodizonate ion also attracts interest due to its luminescence properties.<sup>32</sup> The conjugate base of squaric acid can serve as an electrostatic mimic of negatively charged groups that are common in biology; as a result, derivatives of squaric acid have been used as substitutes for carboxylate, phosphate, mono- and di-esters in a number of medicinal applications.<sup>33</sup> Squaric acid derivatives have been used medically in the treatment of baldness.<sup>34,35</sup> Of particular interest in synthetic crosslinking applications oxocarbon ions, mainly croconate and squarate, have been used as building blocks in supramolecular chemistry, in the design of structures containing  $\pi$ -stacking hydrogen bonded monomeric units.<sup>36-38</sup>

In the present work, we have set out to prepare covalent cross-linked chitosan with the parent squaric acid and ionic cross-linked chitosan with different oxocarbon ions namely, sodium squarate, potassium crotonate and potassium rhodizonate, and pseudo-oxocarbons exemplified by potassium croconate violet. The polymer products have been structurally characterized using infrared and Raman spectroscopy, analytical techniques which have been adopted for the structural evaluation of the crosslinking reactant molecules, and their thermal properties have been evaluated by thermogravimetric analysis (TGA). This work sets out to examine first the preparation and structural characterisation of some novel crosslinked chitosans formed ionically and covalently from members of the oxocarbon family; from this initial study we can then evaluate the structural characteristics of the crosslinked polymers against the parent chitosan and reactant oxocarbons and preliminary studies of the thermal behavior of the materials will enable an assessment to be made of their thermal stabilities which will facilitate future experiments designed to compare the crosslinked polymer resistance to degradation and potentially improved chemical solubility with changes in thermal behavior compared with chitosan itself.

## Experimental

### Materials

Chitosan (medium molecular weight, viscosity: 200-800 cP, 1% wt.% in 1% acetic acid at 25 °C and

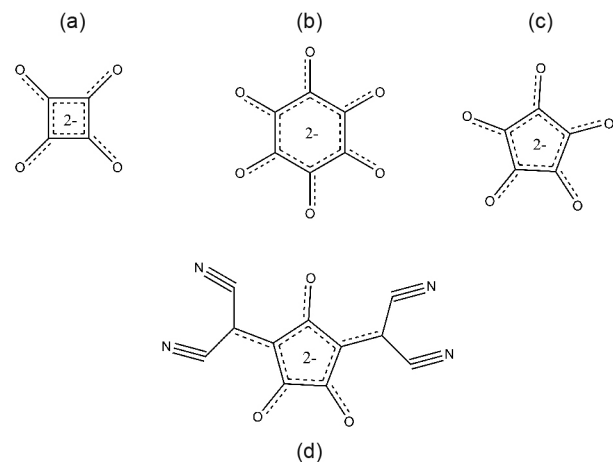


**Figure 1.** Chemical structures of the oxocarbon ions: squarate (a); rhodizonate (b); croconate (c) and croconate violet (d).

soluble in dilute aqueous acid), squaric acid and potassium rhodizonate, were purchased from Sigma Aldrich® and were used without further purification. Methanol solvent was purchased from Vetec®. Sodium squarate was obtained by the neutralization of squaric acid with sodium hydroxide, and potassium croconate<sup>39,40</sup> and potassium croconate violet<sup>41</sup> were synthesized according to the general methods described in the literature. The chitosan used to perform the syntheses was deacetylated using a 20% solution of sodium hydroxide.

### Synthesis of cross-linked chitosan

The synthesis of covalent cross-linked chitosan was performed in a heterogeneous phase using anhydrous methanol as solvent.<sup>42</sup> Chitosan (100 mg), squaric acid (200 mg) and 50 mL of anhydrous methanol were added to a flask and the reaction mixture was refluxed for 24 h, after which the solid deposited was filtered and washed with water and ethanol to remove the oxocarbon excess reactant and vacuum dried. To obtain the ionic cross-linked chitosan, 0.3 g of the polymer was dissolved in 10 mL of a 1% solution of acetic acid. An aqueous solution of oxocarbon 0.75% m/v was added to this viscous solution and the solid obtained was filtered and washed with distilled water to remove the excess of residual oxocarbon, and subsequently vacuum dried. The ionic cross-linked chitosans obtained by using sodium squarate, potassium rhodizonate, potassium croconate violet and potassium croconate were designated: (1), (2), (3) and (4), whereas the covalent cross-linked chitosan obtained with squaric acid was designated as (5). It should be noted that in the procedure using potassium violet croconate, it was not possible to obtain the solid product directly by precipitation; in this case, the solvent was evaporated under reduced pressure and the residue washed with distilled water to remove excess potassium croconate violet and then it was dried.

### Fourier transform infrared spectroscopy

Fourier transform infrared (FTIR) spectra were obtained using an ALPHA FT-IR Bruker Spectrometer in the 4000-600 cm<sup>-1</sup> region. The attenuated total reflection method (ATR) was adopted with a resolution of 4 cm<sup>-1</sup> and 64 spectral scans accumulation.

### Raman spectroscopy

Raman measurements were performed using a Bruker RFS 100 instrument excited with a Nd<sup>3+</sup>/YAG laser operating at 1064 nm, equipped with a germanium detector

cooled with liquid nitrogen and operating with a spectral resolution of 4 cm<sup>-1</sup>. An average of 1024 scans were collected for each specimen with a laser power of 200 mW directed at the sample.

### Solid-state nuclear magnetic resonance (NMR)

The <sup>13</sup>C NMR spectra were obtained on a Bruker Advance III spectrometer operating with a field 7.05 T Bruker CPMAS probe using a rotor 4 mm ZrO<sub>2</sub>, and spinning the sample at a frequency of 3 kHz. A sample of glycine was used as internal standard (38.45 ppm) for calibration purposes.

### Thermogravimetric analyses

Thermogravimetric analyses (TG) were performed in a Shimadzu TG-60 instrument under nitrogen atmosphere with a flow of 50.0 mL min<sup>-1</sup> and a heating rate of 10 °C min<sup>-1</sup> from 25 to 550 °C.

## Results and Discussion

The formation of chitosan ionic cross-linked polymers can be observed simply by the increase in the turbidity in aqueous solutions of the appropriate oxocarbon upon the addition of an acidic solution of chitosan. This was observed for all experiments with the exception of the potassium croconate violet cross-linking agent. Thus, it seems that two different mechanisms could be acting: the cross-linking was initially effective by protonation at lower pH, whereas the chitosan-oxocarbon complex at higher pH was formed by the ionic interaction between the positively charged chitosan and the negatively charged oxocarbon ions. In other words, the cross-linking mechanism for the interaction between chitosan and oxocarbon ions could be<sup>43</sup> accomplished either by protonation or by ionic interaction, as shown in Figure 2, where the proposed structures for each of the synthesized compounds containing the oxocarbon species can be seen, namely squarate, croconate and rhodizonate ions as well as the squaric acid.

Infrared spectroscopy was used to analyse the structural changes of the polymers produced after the ionic and covalent crosslinking. The infrared spectra of the samples are shown in Figure 3, and the main vibrational bands are listed in Table 1, together with a tentative assignment based on the literature.<sup>44-47</sup> A characteristic band at ca. 3360 cm<sup>-1</sup> is assigned to the ν(NH<sub>2</sub>) and ν(OH) modes. On comparing the FTIR spectra of chitosan with those cross-linked from (1), (2), (5) and (4), it can be observed that there are modifications in the intensity and a significant broadening

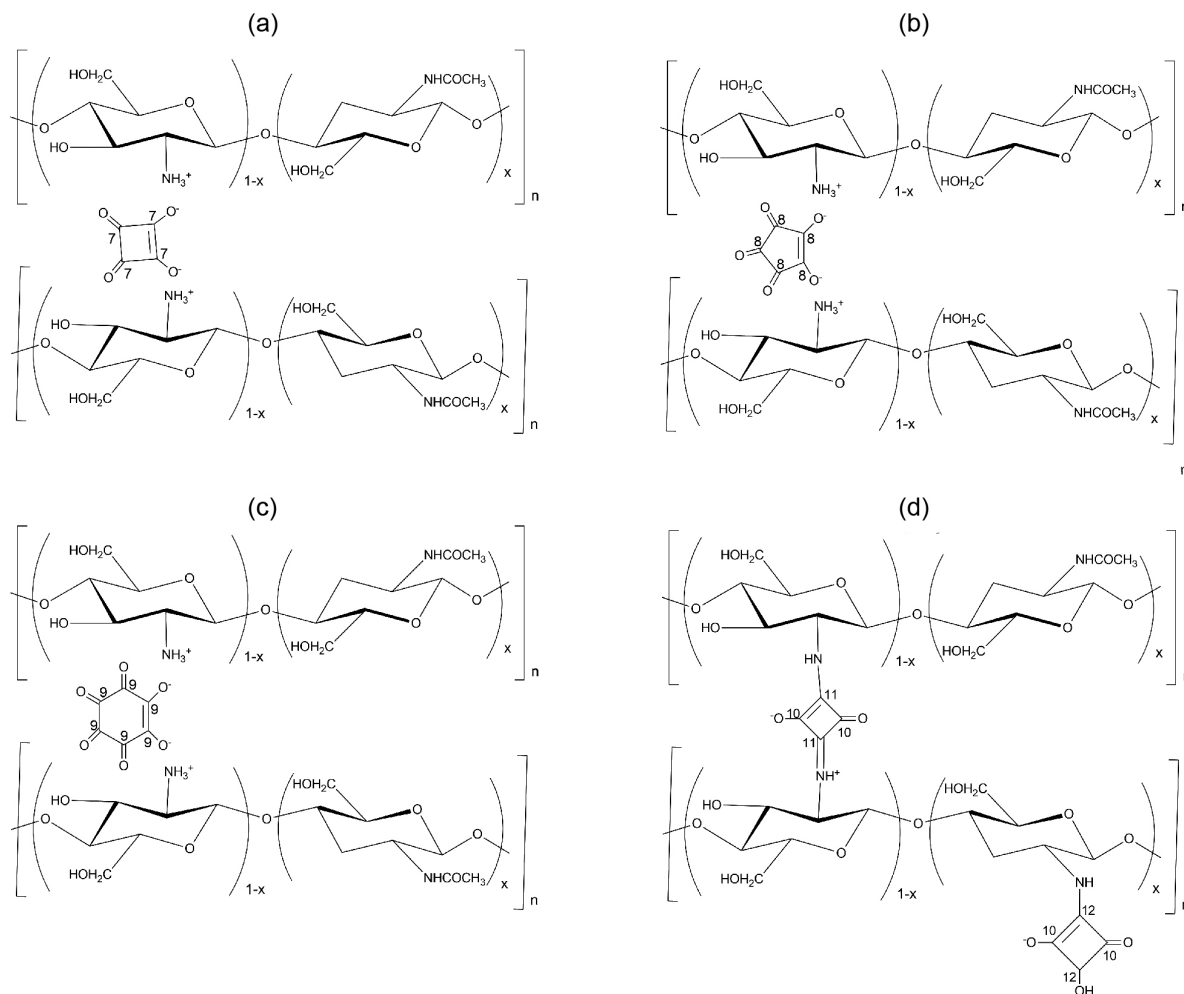


**Figure 2.** Proposed structures for the crosslinked chitosans containing the respective oxocarbon ions.

of several bands, which can be understood as evidence for the molecular interaction between the chitosan chemical functional groups and the oxocarbon ions, mainly occurring via hydrogen bond interactions.<sup>48,49</sup>

For the ionic cross-linked chitosans (1), (2) and (4) the band at  $1650\text{ cm}^{-1}$  assigned to the amide  $\nu(\text{C}=\text{O})$  mode originally observed in the chitosan spectrum, disappears and a new band at  $1645\text{ cm}^{-1}$  appears. This is consistent with literature reports of the absence of the band at  $1650\text{ cm}^{-1}$  and the presence of two bands at ca.  $1640$  and  $1550\text{ cm}^{-1}$ .<sup>49</sup>

The disappearance of this amide band could be attributed to the new bond formed between the oxocarbon ion and the ammonium ions in chitosan, whereas a new band appearing at  $1545\text{ cm}^{-1}$ , assigned to the  $\delta$  mode, can be ascribed to the protonation of the amine group in chitosan.<sup>50</sup> However, it is not possible to verify the presence of the band expected at  $1550\text{ cm}^{-1}$ , possibly because the bandwidth for the oxocarbon absorption band masks it. The band at  $1342\text{ cm}^{-1}$ , assigned to the  $\nu(\text{C}-\text{N})$  mode, is shifted to lower wavenumbers for the (2) and (4) polymers; this

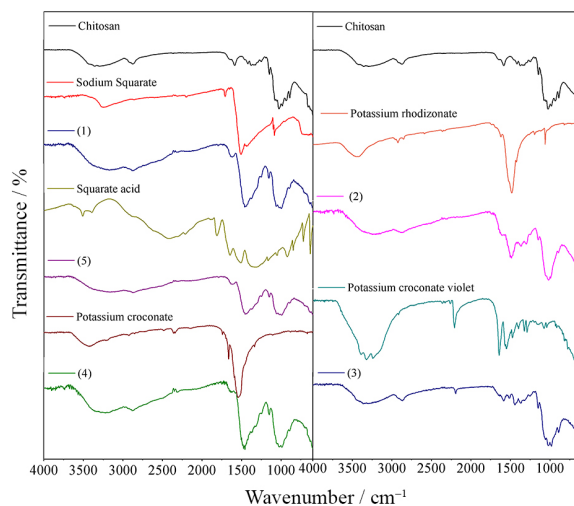


**Figure 3.** Infrared absorption spectra of the indicated samples.

may be attributed to the ionic interaction between chitosan and the oxocarbon ions. This change is not observed for (1), because an oxocarbon vibrational band is present in

the same region at  $1340\text{ cm}^{-1}$ . Similar results were also reported in the literature with phosphate ion.<sup>36,51</sup>

In the infrared spectrum of (5) it is possible to observe changes which are indicative of the presence of covalent cross-linking; for instance, the band at  $1536\text{ cm}^{-1}$ , assigned to the  $\nu(\text{C}=\text{N})$  mode, is characteristic for the formation of the imine group. This band is also observed with chitosan cross-linked with aldehyde which also results in the formation of the imine group.<sup>42,50,52,53</sup> The presence of the band at  $1380\text{ cm}^{-1}$ , assigned to the  $\nu(\text{C}-\text{N}-\text{C})$  mode, also indicates cross-linking due to chemical bond formation between squaric acid and chitosan. It is important to notice that the band at  $1380\text{ cm}^{-1}$ , present in the infrared spectrum of (5), is absent in the (1) spectrum, which clearly indicates that, although the same oxocarbon has been used as a crosslinking agent, two different types of cross-linked chitosan are actually obtained.

According to Figure 3, the infrared spectral analysis of (3) has shown that there are no observed spectral changes for the amine group, one of the most important chemical groups involved in the discussion of ionic cross-linking. The significant difference between this spectrum and the others is the wavenumber position of the band at  $2209\text{ cm}^{-1}$ , assigned to the  $\nu(\text{C}\equiv\text{N})$  mode from the bis(dicyanomethylene) group from croconate violet ion,

which occurs in exactly the same position and intensity when compared to the parent croconate violet salt; this strongly indicates the croconate violet ions are physically rather than chemically adsorbed into the structure of chitosan, which explains the absence of precipitation in the sample preparation compared with the other oxocarbon ions interacting with chitosan.

Raman spectra of the samples are shown in Figure 4, and the main vibrational bands are reported in Table 2, together with a tentative assignment based on the literature.<sup>43-47</sup> In the same way as infrared spectroscopy, Raman spectroscopy has been used to analyse the molecular structures of the cross-linked chitosans. The two most intense bands in the Raman spectra of the oxocarbons are related to the ring breathing and  $\delta(\text{ring})$  (or ring deformation) vibrational modes; these bands are also those most affected by the interaction of the oxocarbons with chitosan, being shifted to lower wavenumbers for both (2) and (1) samples and to higher wavenumbers for (4) and for the (5), where these bands can be seen split into two components (see Table 2).

Such perturbations are a clear demonstration of the existence of interactions between chitosan and the oxocarbon ions, which are responsible for these changes in the vibrational modes of the oxocarbon moieties. The band splitting for C-SquAc can be understood by the formation

**Table 1.** Main infrared wavenumber values (in  $\text{cm}^{-1}$ ) of the samples and respective tentative assignments

Sample											
Chitosan	Sodium squarate	(1)	Squaric acid	(5)	Potassium croconate	(4)	Potassium rhodizonate	(2)	Potassium croconate violet	(3)	Tentative assignment
–	–	–	–	–	–	–	–	–	2209 m	–	$\nu(\text{C}\equiv\text{N})$
–	1707 w	–	1814 m	–	–	–	–	–	1647 m	–	$\nu(\text{C}=\text{O})$
1650 m	–	1617 s	–	1634 w	–	1620 w	–	1612 w	–	1650 w	$\nu(\text{C}=\text{O})$ amide
–	–	–	1646 m	–	–	–	–	–	–	–	$\nu(\text{C}=\text{C})$
1588 m	–	–	–	–	–	–	–	–	–	–	$\delta(\text{NH}_2)$
–	–	–	–	–	–	–	–	–	1566 m 1555 m 1476 m	–	$\nu(\text{C}=\text{O}) + \nu(\text{C}=\text{C}) + \nu(\text{CCCN}_2)$
–	1511 s	1441 s	1540 m	–	1540 s	1466 s	1487 s	1484 s	–	–	$\nu(\text{C}=\text{C}) + \nu(\text{C}=\text{O})$
–	1427 m	1372 s	1328 m	–	–	–	–	–	–	–	$\nu(\text{C}-\text{C})$
1374 m	–	–	–	–	–	1372 w	–	1374 w	–	1372 w	$\delta(\text{CH}_3)$ in amide
1342 w	–	–	–	–	–	1320 w	–	1301 w	–	1342 w	$\nu(\text{CN})$ amine
1250 w	–	1247 w	–	1250 w	–	1247 w	–	1247 w	–	1250 w	$\delta(\text{OH})$ out of plane
1149 m	–	1151 w	–	1152 w	–	1151 w	–	1149 w	–	1149 w	$\nu(\text{C}-\text{O}-\text{C})$ from $\beta(1-4)$ bond
1078 m	–	1066 m	–	1162 w	–	1156 w	–	1156 w	–	1158 w	$\nu(\text{C}-\text{O}-\text{C})$ glucosyl ring
890 w	–	891 w	–	896 w	–	891 w	–	896 w	–	891 w	$\nu(\text{C}-\text{O}-\text{C})$ from $\beta(1-4)$ bond

w: weak; m: medium; s: strong.

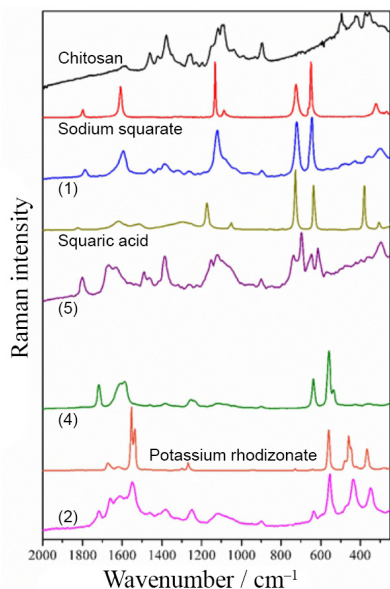


**Figure 4.** Raman spectra excited at 1064 nm of the indicated samples.

of new covalent bonds which cause a significant change in some vibrational modes by affecting the force constants for several different bonds in the structure of the polymer. It is also possible to verify other spectral changes, such as the bands assigned to the oxocarbon  $\nu(\text{C}=\text{O})$  mode, which

are shifted to lower wavenumbers; this band shift is more pronounced for the C-AcSqu sample, probably due to the formation of covalent bonds which most effectively modify this vibrational mode.

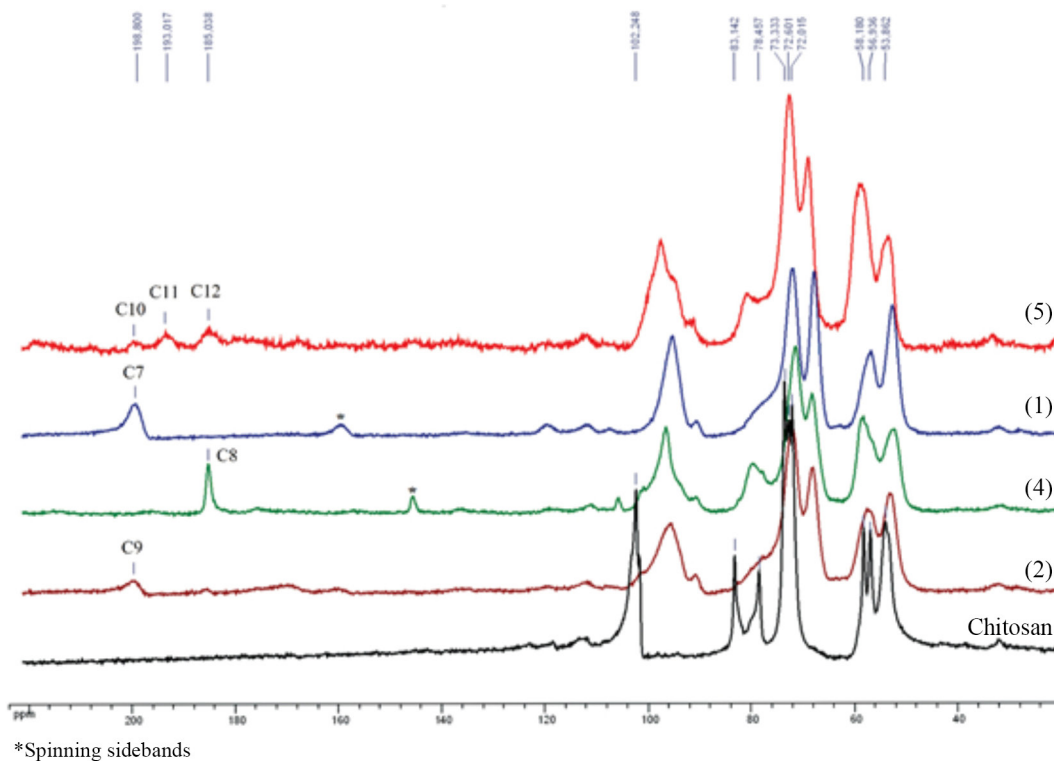
The bands assigned to the oxocarbon  $\nu(\text{C}=\text{C})$  mode are also shifted to lower wavenumbers, and in particular for the C-Cro sample this band now has an asymmetric shoulder, which can be related to more than one  $\text{C}=\text{C}$  bond present in the structures. As for the carbon-carbon double bond modes, the bands assigned to the  $\nu(\text{C}-\text{C})$  mode of the oxocarbon species are shifted to lower wavenumbers for both (1) and (5) samples. Once again, such changes in the oxocarbon vibrational modes are indicative of the interaction and formation of cross-linked polymers. A significant difference between the Raman spectra of (5) and (1) is the presence of bands at 1632 and 1667  $\text{cm}^{-1}$  in the former, which can be assigned to the  $\nu(\text{C}=\text{N})$  mode<sup>37</sup> related to the covalent cross-linked chitosan.<sup>36</sup> It is difficult to analyse the Raman band changes occurring in chitosan upon crosslinking since the oxocarbon Raman bands overlap the weaker intensity features of the chitosan.

Figure 5 shows the comparison between the solid state  $^{13}\text{C}$  NMR spectrum of chitosan with the cross-linked chitosan and the main signals are listed in Table 3, where

**Table 2.** Main Raman wavenumber values (in  $\text{cm}^{-1}$ ) of the samples and respective tentative assignments

Chitosan	Sample								Tentative assignment
	Sodium squarate	(1)	Squarate acid	(5)	Potassium croconate	(4)	Potassium rhodizionate	(2)	
–	1796 w	1784 w	1822 w	1801 w	1722 s	1716 s	1672 s	1659 s	$\nu(\text{C}=\text{O})$
–	–	–	1617 w	1619 s	1606 s	1587/1608 s	–	–	$\nu(\text{C}=\text{C})$
–	1608 s	1593 s	1513 w	–	–	–	–	–	$\nu(\text{C}=\text{C}) + \nu(\text{C}=\text{O})$
1587 w	–	–	–	–	–	–	–	–	$\delta(\text{NH}_2)$
–	–	–	–	–	–	–	1551 s	1549 s	$\nu(\text{C}=\text{O})$
1420 m	–	1418 w	–	1415 w	–	1420 w	–	1411 w	$\delta(\text{CH}_2)$
1377 s	–	1386 w	–	1388 s	–	1382 w	–	1379 w	$\delta(\text{CH}_3)$ in amide
1346 sh	–	–	–	–	–	–	–	–	$\delta(\text{N}-\text{H}), \nu(\text{C}-\text{N})$
–	–	–	1295 w	–	1240 s	1253/1236 w	1267 s	1246 m	$\nu(\text{C}-\text{C})$
1262 m	–	1265 w	–	1621 w	–	–	–	–	$\tau(\text{CH}_2), \delta(\text{HCC}), \delta(\text{HOC}), \delta(\text{COH})$
–	1132 s	1119 s	1172 m	1151 m	–	–	–	–	$\nu(\text{C}-\text{C})$
1039 w	–	1035 sh	–	–	–	–	–	–	$\nu(\text{C}-\text{C}), \nu(\text{C}-\text{O})$
895 s	–	895 w	–	899 w	–	899 w	–	897 w	$\nu(\text{C}-\text{O}-\text{C})$ from $\beta(1-4)$ bond
–	724 s	721 s	726 s	736/696 s	635 s	637	558 s	552 s	Ring breathing
–	649 s	643 s	637 s	645/613 s	554 s	558	480 m	470 sh	$\delta_{\text{ring}}$
–	321 w	298 w	381 s	–	531 sh	535	459 s	736 s	$\delta(\text{CO})$
–	–	–	–	–	–	–	366 s	347 s	$\delta_{\text{ring}}$

w: weak; m: medium; s: strong; sh: shoulder.



**Figure 5.**  $^{13}\text{C}$  NMR (3 kHz) solid of the indicated samples.

also can be seen the chemical shifts based on similar systems.<sup>54-56</sup>

In the solid state  $^{13}\text{C}$  NMR spectra of the samples (2), (1) and (4) it is possible to observe only one signal related to the carbon of the carbonyl group, which is also indicative of the ionic character of the crosslinking for chitosan. Unlike the (5) sample, it is possible to observe the presence of three signals at 199.23, 193.04 and 185.03 ppm; the first signal refers to the carbon of the carboxylic group of squaric acid, whereas the signal at 193.04 ppm is related to the carbons of the squaric acid, which are involved in the covalent crosslinking and the third at 185.03 ppm is related to the non-carboxylic carbons of the squaric acid moiety which are covalently bound to chitosan but not performing the crosslinking. All these data which are closely related to covalently crosslinked chitosan are consistent with similar structures previously investigated in the literature.<sup>57</sup>

An important criterion for technological applications is the thermal stability of the crosslinked polymers and hence TGA analyses of chitosan and crosslinked chitosan were performed; Figure 6a displays the thermogravimetric curves for all the compounds prepared here and the DTG curves are depicted in Figure 6b. The TG curve for chitosan exhibits a thermal degradation in two steps; the first weight loss is due to the loss of adsorbed water, whereas the second degradation step corresponds to the dehydration of the saccharide rings together with a depolymerization/

decomposition of the acetylated and deacetylated units of chitosan, starting from 280 °C and being completed at 380 °C.<sup>44</sup> Some changes in the chitosan degradation temperature can be observed after crosslinking, and all these data are summarized in Table 3.

Through the TG curves, it is possible to note that for the samples (2), (1), (4) and (5), the degradation process starts at a temperature lower than that for chitosan before the crosslinking process. However, for the (3) sample there is no significant change observed in the starting temperature for the thermal degradation. Analysis of the DTG curves shows the temperature where the rate of decomposition is maximum ( $T_{\text{dmax}}$ ); from a comparison of the maximum decomposition temperature of the crosslinked samples and chitosan itself is possible to verify that this maximum temperature is shifted to lower temperatures for all samples, except for (3) where no significant change is observed. The decrease in thermal stability observed by TG and DTG measurements for (1), (5), (2) and (4) must be related to the crosslinking process, thus suggesting that this crosslinking process reduces the chitosan thermal stability. In particular, for the (3) sample, no significant change is observed in the thermal stability; this fact suggests the absence of the crosslinking process for the chitosan polymeric chains, when using potassium croconate violet as crosslinking agent, which is in agreement with the infrared spectroscopic analysis. The absence of a crosslinking process when using

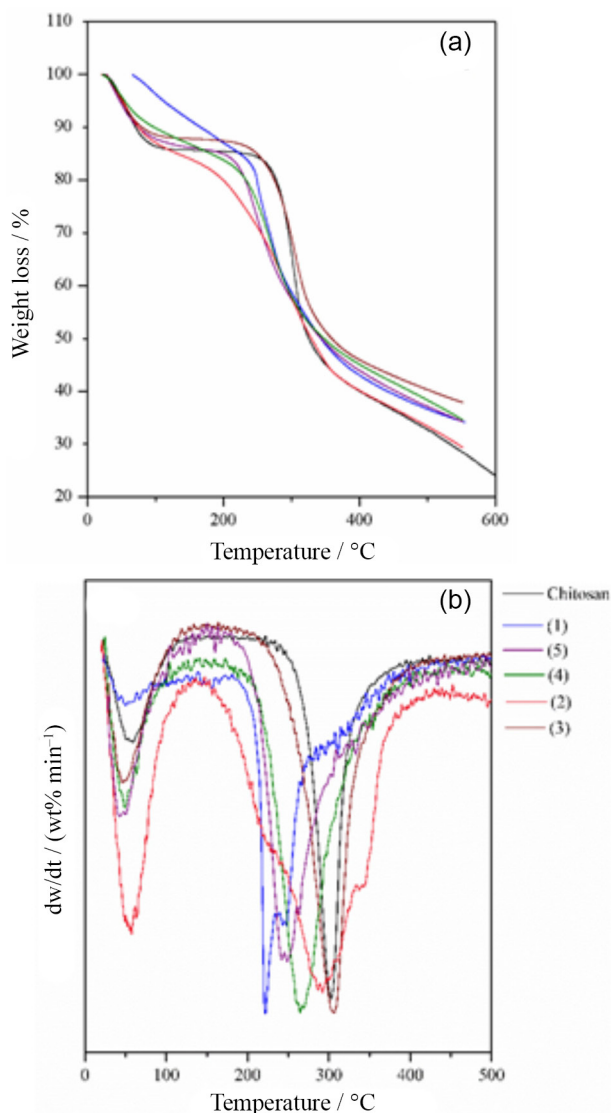


**Figure 6.** Thermogravimetric data: TGA curves (a) and DTG curves (b) of the indicated samples.

**Table 3.** Thermal data of chitosan and cross-linked chitosan

Sample	TG	DTG
	$T_{\text{onset}} / ^\circ\text{C}$	$T_{\text{dmax}} / ^\circ\text{C}$
Chitosan	280	302
(1)	214	221
(5)	224	248
(4)	236	263
(2)	225	286
(3)	272	306

violet croconate can be explained by the low basic strength of the molecule, thus showing that it is not necessary to possess an electrostatic interaction to initiate the ionic crosslinking process.

Summing up, the obtained crosslinked polymers involving chitosan and oxocarbon moieties present a worst thermal characteristic when compared with natural chitosan. Nevertheless, it is important to note that the thermal instability observed for the crosslinked compounds can be related to the chemical composition of such materials, since the thermal stability is mainly related to the chitosan structure, despite how strong is the interaction between the chitosan and the oxocarbon moieties. The comparison is very clear, observing the temperature of decomposition of crosslinked chitosan with other ions, such as phosphate and carboxylic acids.<sup>58,59</sup>

## Conclusions

The present investigation describes the synthesis and characterization of four new crosslinked chitosan polymers. The chitosan crosslinking was performed using different oxocarbon moieties (potassium croconate, potassium croconate violet, potassium rhodizonate, squaric acid and sodium squarate) as crosslinking agents. The oxocarbon salts (potassium croconate, potassium croconate violet, potassium rhodizonate, and sodium squarate) were used in order to obtain the ionic crosslinking chitosans and the parent squaric acid was used to obtain covalent crosslinking chitosan. All the samples were analyzed using infrared spectroscopy, thermal analysis and Raman spectroscopy, in order to analyze the chitosan crosslinking process and its influence on the chemical structure of the polymer, as well as their thermal stability. The solid state  $^{13}\text{C}$  NMR has shown the covalent crosslinking character for the squaric acid polymer. The results confirm the covalent and ionic crosslinking of all polymers but potassium croconate violet, where it is not observed to participate in the crosslinking process. Moreover, for the materials where the crosslinking process was observed, a decrease in the thermal stability of the crosslinked polymer has been observed; besides the improvement of new materials, the specific thermal properties for such compounds is not better than the natural chitosan.

## Acknowledgements

Authors are indebted to CNPq, CAPES, FINEP and FAPEMIG (Brazilian agencies) for financial support.

## References

1. Hejazi, R.; Amiji, M.; *J. Controlled Release* **2003**, *89*, 151.
2. Lu, G.; Kong, L.; Sheng, B.; Wang, G.; Gong, Y.; Zhang, X.; *Eur. Polym. J.* **2007**, *43*, 3807.



3. Berger, J.; Reist, M.; Mayer, J. M.; Felt, O.; Peppas, N. A.; Gurny, R.; *Eur. J. Pharm. Biopharm.* **2004**, *57*, 19.
4. Sorlier, P.; Denuzière, A.; Viton, C.; Domard, A.; *Biomacromolecules* **2001**, *2*, 765.
5. Dong, Y.; Qiu, W.; Ruan, Y.; Wu, Y.; Wang, M.; Xu, C.; *Polym. J.* **2001**, *33*, 387.
6. Chen, C. S.; Liao, W. Y.; Tsai, G. J.; *J. Food Prot.* **1998**, *61*, 1124.
7. Chung, L. Y.; Schmidt, R. J.; Hamlyn, P. F.; Sagar, B. F.; Andrews, A. M.; Turner, T. D.; *J. Biomed. Mater. Res.* **1998**, *39*, 300.
8. Chung, Y. S.; Lee, K. K.; Kim, J. W.; *Text. Res. J.* **1998**, *68*, 772.
9. Denuziere, A.; Ferrier, D.; Damour, O.; Domard, A.; *Biomaterials* **1998**, *19*, 1275.
10. MacLaughlin, F. C.; Mumper, R. J.; Wang, J.; Tagliaferri, J. M.; Gill, I.; Hinchcliffe, M.; Rolland, A. P.; *J. Controlled Release* **1998**, *56*, 259.
11. Nerem, R. M.; *Ann. Biomed. Eng.* **1991**, *19*, 529.
12. Berthod, F.; Saintigny, G.; Chretien, F.; Hayek, D.; Collombel, C.; Damour, O.; *Clin. Mater.* **1994**, *15*, 259.
13. Felt, O.; Furrer, P.; Mayer, J. M.; Plazonnet, B.; Buri, P.; Gurny, R.; *Int. J. Pharm.* **1999**, *180*, 185.
14. Patashnik, S.; Rabinovich, L.; Golomb, G.; *J. Drug Targeting* **1997**, *4*, 371.
15. Song, J.; Suh, C. H.; Park, Y. B.; Lee, S. H.; Yoo, N. C.; Lee, J. D.; Kim, K. H.; Lee, S. K.; *Eur. J. Nucl. Med.* **2001**, *28*, 489.
16. Ueno, H.; Mori, T.; Fujinaga, T.; *Adv. Drug Delivery Rev.* **2001**, *52*, 105.
17. Felt, O.; Carrel, A.; Baehni, P.; Buri, P.; Gurny, R.; *J. Ocul. Pharmacol. Ther.* **2000**, *16*, 261.
18. Liu, X. F.; Guan, Y. L.; Yang, D. Z.; Li, Z.; Yao, K. D.; *J. Appl. Polym. Sci.* **2001**, *79*, 1324.
19. Neto, C. G. T.; Dantas, T. N. C.; Fonseca, J. L. C.; Pereira, M. R.; *Carbohydr. Res.* **2005**, *340*, 2630.
20. Martinez, L.; Agnely, F.; Leclerc, B.; Siepmann, J.; Cotte, M.; Geiger, S.; Couarraze, G.; *Eur. J. Pharm. Biopharm.* **2007**, *67*, 339.
21. He, P.; Davis, S. S.; Illum, L.; *Int. J. Pharm.* **1999**, *187*, 53.
22. Tikhonov, V. E.; Radigina, L. A.; Yamskov, Y. A.; *Carbohydr. Res.* **1996**, *290*, 33.
23. Ngah, W. S. W.; Fatinathan, S.; *Colloids Surf., A* **2006**, *277*, 214.
24. Saha, T. K.; Ichikawa, H.; Fukumori, Y.; *Carbohydr. Res.* **2006**, *341*, 2835.
25. Shu, X. Z.; Zhu, K. J.; *Eur. J. Pharm. Biopharm.* **2002**, *54*, 235.
26. Karakeçili, A. G.; Satriano, C.; Gümüşderelioğlu, M.; Marletta, G.; *J. Appl. Polym. Sci.* **2007**, *106*, 3884.
27. Maguerroski, K. S.; Fernandes, S. C.; Franzoi, A. C.; Vieira, I. C.; *Enzyme Microb. Technol.* **2009**, *44*, 400.
28. Oliveira, V. E.; Freitas, M. C. R.; Diniz, R.; Yoshida, M. I.; Speziali, N. L.; Edwards, H. G. M.; de Oliveira, L. F. C.; *J. Mol. Struct.* **2008**, *881*, 57.
29. Teles, W. M.; Farani, R. A.; Maia, D. S.; Speziali, N. L.; Yoshida, M. I.; de Oliveira, L. F. C.; Machado, F. C.; *J. Mol. Struct.* **2006**, *783*, 52.
30. Lopes, J. G. S.; de Oliveira, L. F. C.; Edwards, H. G. M.; Santos, P. S.; *J. Raman Spectrosc.* **2004**, *35*, 131.
31. de Oliveira, L. F. C.; Santos, P. S.; *J. Mol. Struct.* **1992**, *269*, 85.
32. Oliveira, V. E.; Diniz, R.; de Oliveira, L. F. C.; *Quim. Nova* **2009**, *32*, 1917.
33. Onaran, M. B.; Comeau, A. B.; Seto, C. T.; *J. Org. Chem.* **2005**, *70*, 10792.
34. Case, P. C.; Mitchell, A. J.; Swanson, N. A.; Vanderveen, E. E.; Ellis, C. N.; Headington, J. T.; *J. Am. Acad. Dermatol.* **1984**, *10*, 447.
35. Orecchia, G.; Rabbiosi, G.; *J. Am. Acad. Dermatol.* **1987**, *16*, 876.
36. Ribeiro, M. C. C.; de Oliveira, L. F. C.; Santos, P. S.; *Chem. Phys.* **1997**, *217*, 71.
37. Silva, C. E.; Diniz, R.; Rodrigues, B. L.; de Oliveira, L. F. C.; *J. Mol. Struct.* **2007**, *831*, 187.
38. de Oliveira, C. I. R.; de Oliveira, L. F. C.; Dias Filho, F. A.; Messaddeq, Y.; Ribeiro, S. J. L.; *Spectrochim. Acta, Part A* **2005**, *61*, 2023.
39. de Paula, E. E. B.; Visentin, L. C.; Yoshida, M. I.; de Oliveira, L. F. C.; Machado, F. C.; *Polyhedron* **2011**, *30*, 213.
40. Seitz, G.; Imming, P.; *Chem. Rev.* **1992**, *92*, 1227.
41. Mathew, S.; Paul, G.; Shivasankar, K.; Choudhury, A.; Rao, C. N. R.; *J. Mol. Struct.* **2002**, *641*, 263.
42. Monier, M.; *Int. J. Biol. Macromol.* **2012**, *50*, 773.
43. Oliveira, L. F. C.; Santos, P. S.; *J. Mol. Struct.* **1991**, *263*, 59.
44. Souza, N. L. G. D.; Brandão, H. M.; de Oliveira, L. F. C.; *J. Mol. Struct.* **2011**, *1005*, 186.
45. Georgopoulos, S. L.; Diniz, R.; Yoshida, M. I.; Speziali, N. L.; Santos, H. F. D.; Junqueira, G. M. A.; de Oliveira, L. F. C.; *J. Mol. Struct.* **2006**, *794*, 63.
46. Diniz, R.; de Sá, L. R. V.; Rodrigues, B. L.; Yoshida, M. I.; de Oliveira, L. F. C.; *Inorg. Chim. Acta* **2006**, *359*, 2296.
47. Junqueira, G. M. A.; Rocha, W. R.; de Almeida, W. B.; dos Santos, H. F.; *J. Mol. Struct.: THEOCHEM* **2004**, *684*, 141.
48. Yuan, Q.; Shah, J.; Hein, S.; Misra, R. D. K.; *Acta Biomater.* **2010**, *6*, 1140.
49. Zhang, L.; Kosaraju, S. L.; *Eur. Polym. J.* **2007**, *43*, 2956.
50. Gupta, K. C.; Jabrail, F. H.; *Carbohydr. Res.* **2006**, *341*, 744.
51. Teles, W. M.; Farani, R. A.; Speziali, N. L.; Yoshida, M. I.; de Oliveira, L. F. C.; Machado, F. C.; *Inorg. Chim. Acta* **2006**, *359*, 3384.
52. Monier, M.; Ayad, D. M.; Abdel-Latif, D. A.; *Colloids Surf., B* **2012**, *94*, 250.

53. Pratt, D. Y.; Wilson, L. D.; Kozinski, J. A.; *J. Colloid Interface Sci.* **2013**, 395, 205.
54. Capitani, D.; de Angelis, A. A.; Crescenzi, V.; Masci, G.; Segre, A. L.; *Carbohydr. Polym.* **2001**, 45, 245.
55. Chen, C.-Y.; Chang, J.-C.; Chen, A.-H.; *J. Hazard. Mater.* **2011**, 185, 430.
56. Webster, A.; Halling, M. D.; Grant, D. M.; *Carbohydr. Res.* **2007**, 342, 1189.
57. de Angelis, A. A.; Capitani, D.; Crescenzi, V.; *Macromolecules* **1998**, 31, 1595.
58. Pieróg, M.; Ostrowska-Czubenko, J.; Gierszewska-Drużyńska, M.; *Progress in the Chemistry and Application of Chitin and its Derivatives (PCACD)* **2012**, 17, 67.
59. Pieróg, M.; Ostrowska-Czubenko, J.; Gierszewska-Drużyńska, M.; *Progress in the Chemistry and Application of Chitin and its Derivatives (PCACD)* **2010**, 15, 25.

Submitted: January 8, 2015

Published online: April 10, 2015